



Marco Donatelli*



Claudio Estatico†



Stefano Serra-Capizzano‡

Abstract

We consider the classical de-blurring problem of noisy and blurred signals or images in the case of space invariant point spread function (PSF) imposing the boundary conditions (BCs). Our focus is on the anti-reflective BCs since they reduce substantially artifacts called ringing effects with respect to other classical choices holding the same computational cost.

The Boundary Conditions

Basically, the mathematical model of image blurring with spatial invariant kernel is the following Fredholm operator of first kind

$$g(x, y) = \int_{\mathbb{R}^2} \mathcal{K}(x - \theta, y - \xi) f_o(\theta, \xi) d\theta d\xi + \nu(x, y),$$

where f_o is the (true) input object, \mathcal{K} is the integral kernel of the operator, also called point spread function, ν is the noise, and g is the observed image.

In the discrete case the observed image is $n \times n$ (for simplicity we assume square images) and the PSF is $p \times p$. It gives rise to the corresponding matrix operator $\mathbf{g} = \mathbf{K}\mathbf{f}_o + \boldsymbol{\nu}$ that is under-determined since the matrix \mathbf{K} has size $n^2 \times m^2$ with $m = n + p - 1$. An attractive technique both from the quality of the restored images and computational point of view is the use of appropriate *boundary conditions*: linear or affine relations between the unknowns outside the field of view (FOV) and the unknowns inside the FOV. The more common type of BCs and related properties are summarized in the following table for the 1D case:

Type	Description outside the FOV	Matrix structure	Matrix-vector product	Ref.
Zero Dirichlet	zero pad	Toeplitz	$O(m \log m)$ complex op.	[1]
Periodic	circular repetition	Circulant	$O(n \log n)$ complex op.	[1]
Reflective	reflection like a mirror	Toeplitz + Hankel	symmetric PSF: $O(n \log n)$ real op. generic: $O(m \log m)$ complex op.	[2]
Anti-reflective	reflection using central symmetry	Toeplitz + Hankel + rank 2	symmetric PSF: $O(n \log n)$ real op. generic: $O(m \log m)$ complex op.	[5]

Table 1. Features of the Boundary Conditions in the 1D case

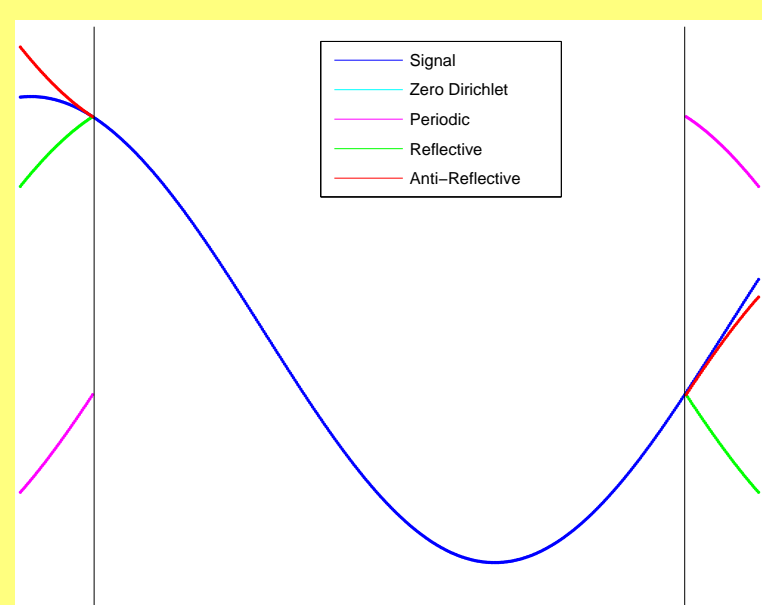


Figure 1. A signal with BCs

The generalization to the d -dimensional case can be done resorting to tensor product argumentations. The computational cost is related to the algebraic actual size of the involved objects (for instance we have $O(n^d \log n)$ for the periodic BCs, if the object is $\underbrace{n \times n \times \dots \times n}_d$).

The Antireflective BCs (AR-BCs)

For the sake of simplicity we explain the imposition of AR-BCs in the 1D case. We emphasize that in the 2D there is not a unique choice at the vertices of the image (see [3]).

Let $\mathbf{f}_0 = (\dots, f_0, f_1, \dots, f_n, f_{n+1}, \dots)^T$ and $\mathbf{h} = (\dots, 0, 0, h_{-p}, h_{-p+1}, \dots, h_0, \dots, h_{p-1}, h_p, 0, 0, \dots)^T$, with $\sum_{j=-p}^p h_j = 1$, be the original signal and the blurring function. We set

$$f_{1-j} = f_1 - (f_{j+1} - f_1) = 2f_1 - f_{j+1}, \quad f_{n+j} = f_n - (f_{n-j} - f_n) = 2f_n - f_{n-j},$$

for $j = 1, \dots, p$. Then $\mathbf{K}\mathbf{f}_0 = \mathbf{g}$ becomes $\mathbf{A}\mathbf{f} = \mathbf{g}$, with $\mathbf{A} \in \mathbf{R}^{n \times n}$. The matrix \mathbf{A} is a Toeplitz+Hankel plus 2 rank correction matrix, where the correction is placed at the first and the last columns. Furthermore, in the case of symmetric PSF, \mathbf{A} belongs to a matrix algebra denoted by \mathcal{S}_1 , such that there exists an algorithm that solves the linear system $\mathbf{A}\mathbf{f} = \mathbf{g}$ in $O(n \log(n))$ operations mainly using the discrete fast sine transforms (DST-Is). The matrix algebra \mathcal{S}_1 can be introduced as follows (see [4]). Let $\mathbf{Q} = \mathbf{Q}_n$ be the n -by- n orthogonal and symmetric matrix expressed by $[Q]_{i,j} = \sqrt{\frac{2}{n+1}} \sin\left(\frac{ji\pi}{n+1}\right)$, $i, j = 1, \dots, n$, then we define $\tau_n = \{QDQ : D \text{ is a real diagonal matrix of size } n\}$. Now, by definition, $M \in \mathcal{S}_1$ if

$$M = \begin{bmatrix} \alpha & & & \\ & \mathbf{v} & \hat{M} & \mathbf{w} \\ & & & \beta \end{bmatrix},$$

with $\alpha, \beta \in \mathbf{R}$, $\mathbf{v}, \mathbf{w} \in \mathbf{R}^{n-2}$ and $\hat{M} \in \tau_{n-2}$.

The previous considerations can be generalized to the d -dimensional case obtaining the \mathcal{S}_d algebra.

The normal equations and re-blurring

Regularization methods extensively used in the literature (e.g., Tikhonov regularization, CGNE, Landweber) are usually applied to the normal equations $A^T \mathbf{A}\mathbf{f} = A^T \mathbf{g}$, with $A \in \mathbf{R}^{n^2 \times n^2}$ in the image deblurring. For the first three kinds of BCs of Table 1, the algebraic transposition of the coefficient matrix can be equivalently obtained by a 180° rotation of the PSF. This fails only in the case of AR-BCs and indeed they lose their supremacy with respect to the other BCs when are applied to the normal equations.

Therefore, instead of dealing with the normal equations, we work with $A' \mathbf{A}\mathbf{f} = A' \mathbf{g}$ where A' is the matrix obtained imposing the current BCs to the transpose of the PSF (the only difference is in the AR-BCs case).

With this new formulation the AR-BCs become again the better choice regarding the quality of the restored

image. This technique is known as *re-blurring* (see [4]). The strategy is useful from a computational point of view as well, since $A' \in \mathcal{S}_2$ (notice that, $A^T A \notin \mathcal{S}_2$ in general, while $A' A \in \mathcal{S}_2$, keeping the $O(n^2 \log(n))$ computational cost for solving the linear system in the case of centro-symmetric PSF).

Numerical experiments

We test the BCs deblurring techniques for the following two shift-invariant 256×256 PSFs.

(I) *Gaussian PSF*. The matrix A is the Kronecker product of two symmetric banded Toeplitz matrices $[T_n]_{r,s} = a_{r-s} = 4k_{0.15}(x_r - x_s)/51$, for $|r - s| < 9$, and 0 elsewhere. $k_\sigma(t)$ is the Gaussian distribution with zero mean and standard deviation σ , and the points x_j for $j = 1, \dots, n$ are equispaced in $[-2, 2]$. The PSF have been proposed by L. Eldén as prototype of image restoration problems.

(II) *Experimental PSF*. The matrix A is the symmetric version, that is, $A = (B + B^T)/2$, of the widely used experimental 256×256 blurring matrix B developed by US Air Force Phillips Laboratory, Lasers and Imaging Directorate, Kirtland Air Force Base, New Mexico.



Figure 2. Experimental PSF, true and observed images

The true data \mathbf{f}_o is either the actor in the middle of Fig. 2 or an image of “blocks of flats”. The noise on the blurred images is Gaussian with zero mean. We recover the 192×192 internal portion of the true data \mathbf{f}_o from the knowledge of the blurred and noisy image in the same area.

Table 2 shows the best relative restoration errors among the first 100 iterations of the CG method.

On the left, both the two input images with signal to noise ratio (SNR) equals to 25 are considered.

On the right, the image of the face of actor for different levels of noise on the blurred data is considered. Although some positive effects arise in all cases, the choice of the anti-reflective BCs is important mainly if the noise on the data is low, that is, for high values of SNR.

Figure 3 shows the three optimal deblurred images, for different BCs.

PSF	Gaussian		Experimental		
	Actor	Blocks of flats	Actor	Blocks of flats	
Image					
Periodic	0.1980	0.3320	0.3609	0.4825	
Reflective	0.1383	0.3040	0.2519	0.3875	
Anti-Ref.	0.1359	0.2941	0.1968	0.3101	

SNR = 25

SNR	Gaussian			Experimental		
	Periodic	Reflective	AR	Periodic	Reflective	AR
5	0.2072	0.1691	0.1775	0.3643	0.2767	0.3403
10	0.2006	0.1575	0.1612	0.3617	0.2632	0.2762
25	0.1980	0.1383	0.1359	0.3609	0.2519	0.1968
50	0.1980	0.1354	0.1318	0.3609	0.2499	0.1907
∞	0.1980	0.1354	0.1318	0.3609	0.2500	0.1907

Actor

Table 2. Best relative restoration errors within 100 iterations of CG method applied to $A' \mathbf{A}\mathbf{f} = A' \mathbf{g}$

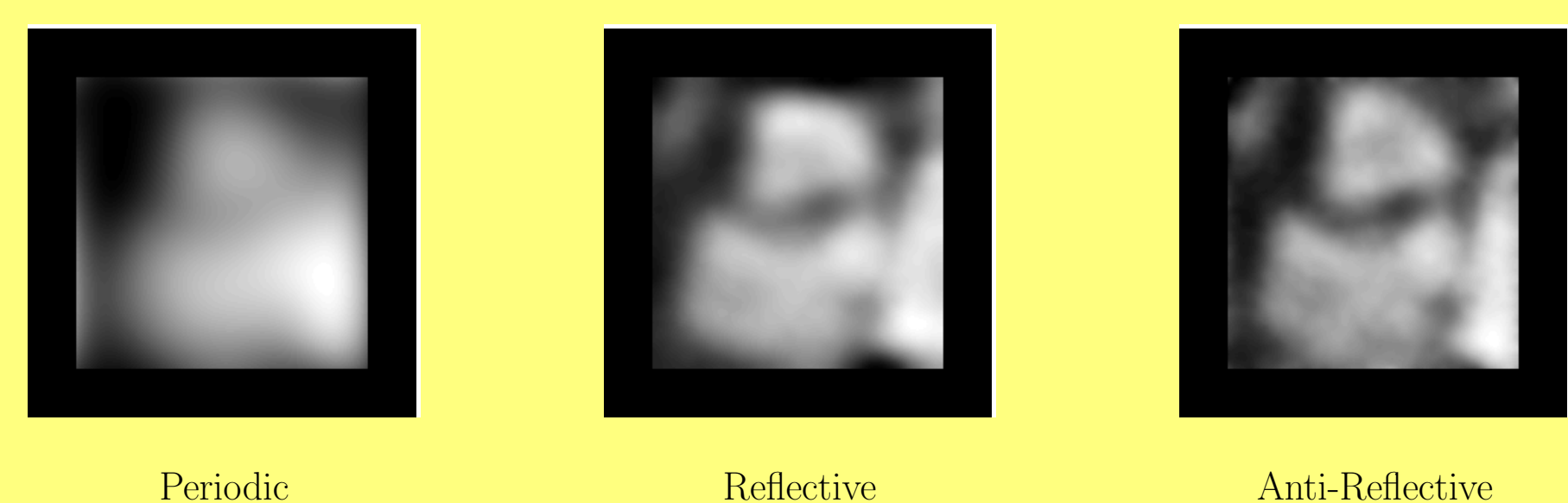


Figure 3. Best restorations for the Experimental PSF

Graphs of convergence histories are plotted in Figure 4. They show the relative restoration errors vs. the iteration number: on the left, the Gaussian PSF; on the right, the Experimental PSFs. In any case, the Anti-Reflective BCs provide the best results and the corresponding curves are quite flat. This way, the estimation of the stop iteration, which generally is a difficult task, is more simple with AR BCs.

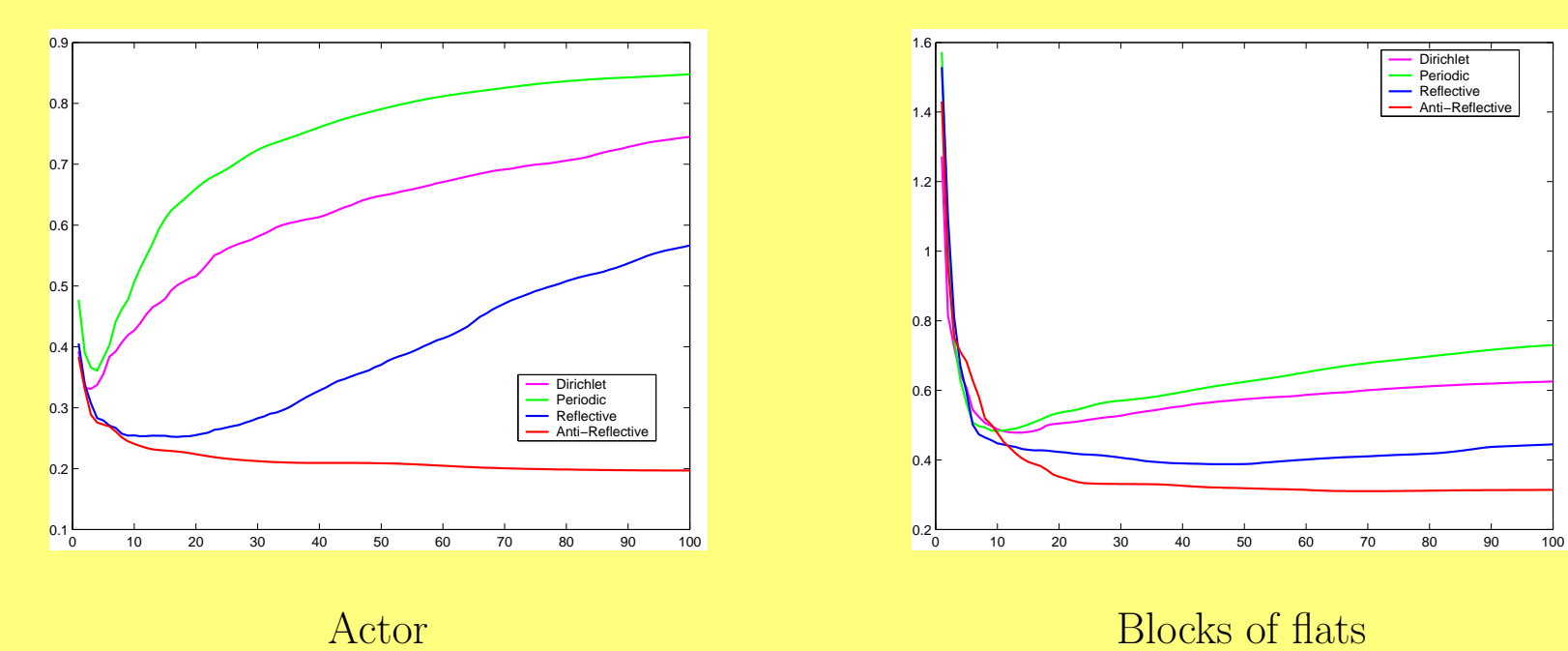


Figure 4. Relative restoration errors vs iteration number for the Experimental PSF

References

- [1] M. Bertero and P. Boccacci 1998, *Introduction to inverse problems in imaging*, Inst. of Physics Publ. Bristol and Philadelphia, London, UK.
- [2] M. Ng, R. H. Chan, and W. C. Tang 1999, A fast algorithm for deblurring models with Neumann boundary conditions, *SIAM J. Sci. Comput.*, 21, pp. 851–866.
- [3] M. Donatelli, C. Estatico, J. Nagy, L. Perrone and S. Serra-Capizzano, Anti-reflective boundary conditions and fast 2D deblurring models, *SPIE's 48th Annual Meeting*, August 2003 in San Diego, CA USA, F. Luk Ed, Vol. 5205 pp. 380–389.
- [4] M. Donatelli and S. Serra Capizzano 2005, Anti-reflective boundary conditions and re-blurring, *Inverse Problems*, 21 pp. 169–182.
- [5] S. Serra Capizzano 2003, A note on anti-reflective boundary conditions and fast deblurring models, *SIAM J. Sci. Comput.*, 25, pp. 1307–1325.

*Dipartimento di Fisica e Matematica, Università dell'Insubria - Sede di Como, Via Valleggio 11, 22100 Como, Italy (marco.donatelli@uninsubria.it).

†Dipartimento di Matematica, Università di Genova, Via Dodecaneso 35, 16146 Genova, Italy (estatico@dim.unige.it).

‡Dipartimento di Fisica e Matematica, Università dell'Insubria - Sede di Como, Via Valleggio 11, 22100 Como, Italy (stefano.serra@uninsubria.it, serra@mail.dm.unipi.it).